https://rbgeomorfologia.org.br/
ISSN 2236-5664

Revista Brasileira de Geomorfologia

v. 23, nº 2 (2022)

http://dx.doi.org/10.20502/rbg.v23i2.2094

Artigo de Pesquisa

A methodological proposal for planation surfaces mapping

Uma proposta metodológica para o mapeamento de superfícies de aplanamento

José Roberto Mantovani [1], Guilherme Taitson Bueno [2]

[1] UNESP, Desastres Naturais, São José dos Campos-SP, Brasil. jr.mantovani.geo@gmail.com.
ORCID: https://orcid.org/0000-0002-7051-5304

[2] UFG, Geografia, Goiânia-GO, Brasil. gtaitson@ufg.br.
ORCID: https://orcid.org/0000-0003-4259-7354

Recebido: 02/02/2021; Aceito: 23/02/2022; Publicado: 06/04/2022

Abstract: A mapping methodology of planation surfaces based on automated altimetric stratification is proposed in this work. In this methodology, mathematical concepts related to the variation of the function of pixels frequency vs. altitude are used to obtain the grouping of relief forms. The automatic clustering allows to distinguish the planation surfaces from elevation without the interference of decision maker. The input data for the execution of the mapping algorithm is the variation of elevation as a function of the number of pixels, extracted from SRTM data. The mapping of planation surfaces and the validation of computational algorithm were carried out for an area located in the municipality of Chapada Gaúcha, Minas Gerais State, Brazil, which presents two planation surfaces recognized in the literature. The landforms in the study area were associated with three planation cycles, interpreted as corresponding to King's Post-Gondwana, South American and Velhas surfaces. Remaining (reserved) and dissected landforms from South American and Velhas surfaces were mapped, while for Post-Gondwana surface only dissected landforms were identified. The mapped surfaces showed an important correlation with the regional soil types, indicating that the spatial distribution of surficial formations is directly related to the distribution of the planation surfaces. The results showed that the proposed algorithm can automatically reveal the relief organization of a region, indicate characteristics of the planation surfaces such as the degree of flatness and leveling, in addition to helping to understand the relationship between landforms and soil distribution. The method is suitable for tectonically stable not-tilted reliefs and for areas of stepped planation surfaces. The method is suitable for stepped landsurfaces located at tectonically stable and not-tilted areas.

Keywords: Planation Surfaces mapping; Geomorphometry; Clustering Algorithm.

Resumo: Este trabalho propõe uma metodologia de mapeamento de superfícies de aplanamento baseada na estratificação altimétrica automatizada. Nesta metodologia, conceitos matemáticos relacionados ao comportamento de variação da função frequência de *pixels* pela altitude são utilizados para obter o agrupamento das formas do relevo. A determinação automática dos grupos de dados permite distinguir as superfícies de aplanamento a partir de dados de elevação sem a interferência do tomador de decisões. O dado de entrada para a execução do algoritmo de mapeamento é a variação da elevação em função do número de *pixels*, extraídos dos dados do SRTM. O mapeamento das superfícies de aplanamento e a validação do algoritmo computacional foram realizados para uma área localizada no município de Chapada Gaúcha, Estado de Minas Gerais, Brasil, que apresenta duas superfícies de aplanamento reconhecidas na literatura. As formas de relevo da área de estudos foram associadas a três ciclos de aplanamento, interpretados como correspondentes às superfícies Pós-Gondwana, Sul Americana e Velhas, de King. Foram mapeadas formas remanescentes (preservadas) e dissecadas das superfícies Sul-Americana e Velhas, enquanto para a superfície Pós-Gondwana foram mapeadas apenas formas dissecadas. As superfícies mapeadas apresentaram importante correlação com os tipos de solo regionais, indicando que a distribuição espacial das formações superficiais está

diretamente relacionada à distribuição das superfícies de aplanamento. Os resultados demonstraram que o algoritmo proposto pode revelar, de forma automatizada, a organização do relevo de uma região, indicar características das superfícies de aplanamento como grau de aplanamento e nivelamento, além de auxiliar na compreensão da relação entre formas de relevo e a distribuição dos tipos de solos. O método proposto é adequado para áreas com superfícies de aplanamento escalonadas, situadas em regiões tectonicamente estáveis e que não sofreram basculamento.

Palavras-chave: Mapeamento de superfícies de aplanamento; Geomorfometria; Algoritmo de clusterização.

1. Introduction

The planation surfaces are conspicuous landforms of earth surface, which are widespread in all continents. They can be morphologically defined as extensive and nearly flat topographical surfaces with low slope gradients, where some residual relief may be present (GOUDIE, 2004). They can be very old in the tectonically stable regions of the globe, with ages back to Cretaceous, even older. In some regions, two or more planation surfaces may exist, on different altitudes and with different ages, forming stepped landscapes. Many million years are necessary for the formation of the planation surfaces (OLLIER; PAIN, 2000). They are formed by erosion to a base level, usually the sea level, during periods of tectonic stability (OLLIER; PAIN, 2000). Planation surfaces may be more or less preserved, according to the degree of fluvial processes (GUILLOCHEAU et al., 2018). For highly dissected surfaces, the former planation surface is sometimes preserved as flat-topped remnants (GUILLOCHEAU et al., 2018) or even as accordant hill summits (OLLIER; PAIN, 2000;).

The issue of planation surfaces is an ancient one in geomorphology, as these landforms have been studied and mapped since the 19th century. Their recognition and mapping were made mostly from topographic maps and fieldworks, with the limitations resulting from the altimetric imprecisions and differences in scale of the topographic maps and, mostly, from the strong influence of the cartographer interpretations and decisions. These drawbacks rendered the planation surface mapping speculative and irreproducible. During the first half of the 20th century, the planation surfaces and the long-term relief evolution were major themes of geomorphology. In the second half of the last century these themes were placed in the background by the interest on more restricted temporal and spatial scales and on the geomorphic processes. More recently, the development of the new geotechnologies as the GPS (Global Positioning System), the GIS (Geographic Information System) and the new isotopic geochronological methods brought a new momentum in long-term and broad scale relief investigation (VASCONCELOS and CARMO., 2018; FREYSSINET et al., 2018; ALLARD et al., 2018). The global Digital Elevation Models allowed access to universal topographic data for any region of the globe and their processing originated numerous proposals for altimetric segmentation aiming the relief compartmentation and the identification of planation surfaces.

Among the works in the literature that address this line of research are those from Macmillan et al. (2000); Jordan (2003); Miliaresis and Iliopoulou (2004); Saadat et al., (2008); Krohling et al., (2014); Leonardi (2014); Bessin et al., (2015); Mokarram e Sathyamoorthy (2016). The main methods for planation surface mapping, proposed by these author are based on the classification of terrain parameters such as hypsometry, slope, aspect, shape and roughness) and on the techniques of filtering by reclassification from DEMs or DTMs (Digital Terrain Model), altimetric clustering (density-slice), TPI (Topographic Position Index) (GUISAN et al., 1999), SOM (clustering of landforms using self-organizing maps) (MOKARRAM e SATHYAMOORTHY, 2016) and LPI (Landform Planation Index) (XIONG et al., 2017). Liu et al., (2019), for example, combined the fuzzy logic from a DEM and the analysis of topographic and long river profiles, focusing on four morphometric parameters (slope, curvature, roughness index and relative height) to propose the relevant fuzzy pertinence functions. The method has, as principle, the idea that flat tops reliefs that stand out from the surroundings have high pertinence (adhesion degree) of belonging

to a planation surface. In this method, the fuzzy logic was used to convert the parameters magnitude into the pertinence of each pixel to pertain to a planation surface (LIU et al., 2019).

The recognition of planation surfaces and of their spatial distribution gives the researcher a first framework for the landscape and environment structure at regional scale and allows genetic interpretations. Besides that, the planation surfaces can be considered important markers for landscape evolution, constituting starting points for the following landscape evolution (COLTORTI and PIERUCCINI, 2000; OLLIER, 2000). The geomorphological and environmental studies starting from the identification and mapping of planation surfaces can be particularly utile for the areas of the globe that were less explored and where the access is difficult.

In this study we propose a method for planation surface identification and mapping based strictly on elevation data. Therefore, it is more appropriate for the tectonically stable regions, with no recent vulcanism, orogenesis and tilted landforms. Even for these regions, one must always consider the limitations of the use of elevation data imposed by the natural slope of planation surfaces and by the effect of regional scale differential tilting, subsidence and uplift. In the proposed planation surface classification and mapping, the expression "planation surface" is employed in a broad and genetic way, assembling all the landforms derived from a former flat surface associated to a planation cycle, i.e., grouping both its flat and near-flat remnants and its dissected areas.

The purpose of this work is to integrate automated techniques for planation surface mapping, by means of an algorithm, as an alternative to manual or analogical methods. The proposed method starts from a SRTM (Shuttle Radar Topography Mission) digital elevation model (MILIARESIS and ILIOPOULOU, 2004) and automatically segments the relief according to the behaviour of the variation of functions (LEITHOLD, 1989). The procedures are based on the analysis of the frequency of pixels as a function of the altitude data extracted from a DEM obtained from SRTM data. Thus, the method automatically determines altitude clusters, allowing to distinguish the planation surfaces and their associated dissected reliefs. This method was developed adopting as study area a region in Minas Gerais State, Brazil, that presents two net planation surfaces, allowing a better calibration of the proposed algorithm.

2. Environmental settings

The study area covers a rectangle of 47 km by 43 km, located in the northwest of Minas Gerais State, in Brazil, with approximately 2,000 km² (Figure 1). Its geological substrate is composed by the Proterozoic arcosean sandstones and siltstones from Três Marias Formation (Bambuí Group), by the Cretaceous sandstones from Areado and Urucuia Groups, by the Neogenic lateritic covers with iron duricrusts and by the Quaternary alluvial deposits (RADAMBRASIL, 1982).

The regional relief is dominated by two stepped planation surfaces recognized in the literature. The uppermost surface is formed by discontinuous tablelands (*chapadas*) whose flat tops remain around 840-880 m a.s.l in the region (Figure 2). This surface is associated to King's South American surface by some authors (BRAUN, 1970; VALADÃO, 2009; LANZA; LADEIRA, 2013) and the perfection of its flatness is in accordance with a period of formation of more than 50 Ma (Upper Cretaceous to Miocene) (KING, 1956; BRAUN, 1970; VALADÃO, 2009). The South American surface is recognized throughout the Brazilian territory and in other parts of South America (RABASSA, 2014). This surface is covered in many parts by a thick regolith with important supergene ore deposits and is capped by mature lateritic crusts (BRAUN, 1970; COSTA, 1991; VASCONCELOS et al., 1994; VALADÃO, 2009). Residual reliefs of ancient planation cycles stand out on some areas of the South American surface (BRAUN, 1970; LANZA; LADEIRA, 2013). In the NW of Minas Gerais, the river valleys on the South American Surface are open and shallow and compose an ancient and low-density drainage network.

The other surface occupies most of the studied region. It is associated to King's *Velhas* Surface (BRAUN, 1970; LANZA; LADEIRA, 2013) or to its equivalent Sul-Americana I surface (VALADÃO, 2009) (Figure 2). This surface does not have the planation degree of South American surface. It presents heterogeneous texture on radar images (VALADÃO, 2009) and is described, for the NW of Minas Gerais, as a surface with undulating relief (AUGUSTIN et al., 2009; VALADÃO, 2009). This may be attributed to factors such as a shorter time of formation (Middle Miocene-Pliocene or ~8 Ma according to VALADÃO, 2009) and the absence of a protective mature lateritic crust. The *Velhas* surface is embedded in South American surface and present relictual hills or *mesas* of this surface (Figure 2). *Velhas* surface areas present a gentle slope towards local or regional base levels (VALADÃO, 2009). The drainage network is denser than that of South American surface. In the studied area, the valleys present *veredas* (*dambo*-like valleys), with swamps and hydromorphic soils. The *vereda* valleys were formed by geochemical losses controlled by geological structures (LIMA; QUEIROZ NETO, 1996; MELO, 2008). Today, the *vereda* landscapes remain mostly in the upper course of the valleys, as the region is undergoing an upstream process of rejuvenation, indicated by the presence of relicts of hydromorphic soils in the already incised segments of the valleys (MELO, 1992).

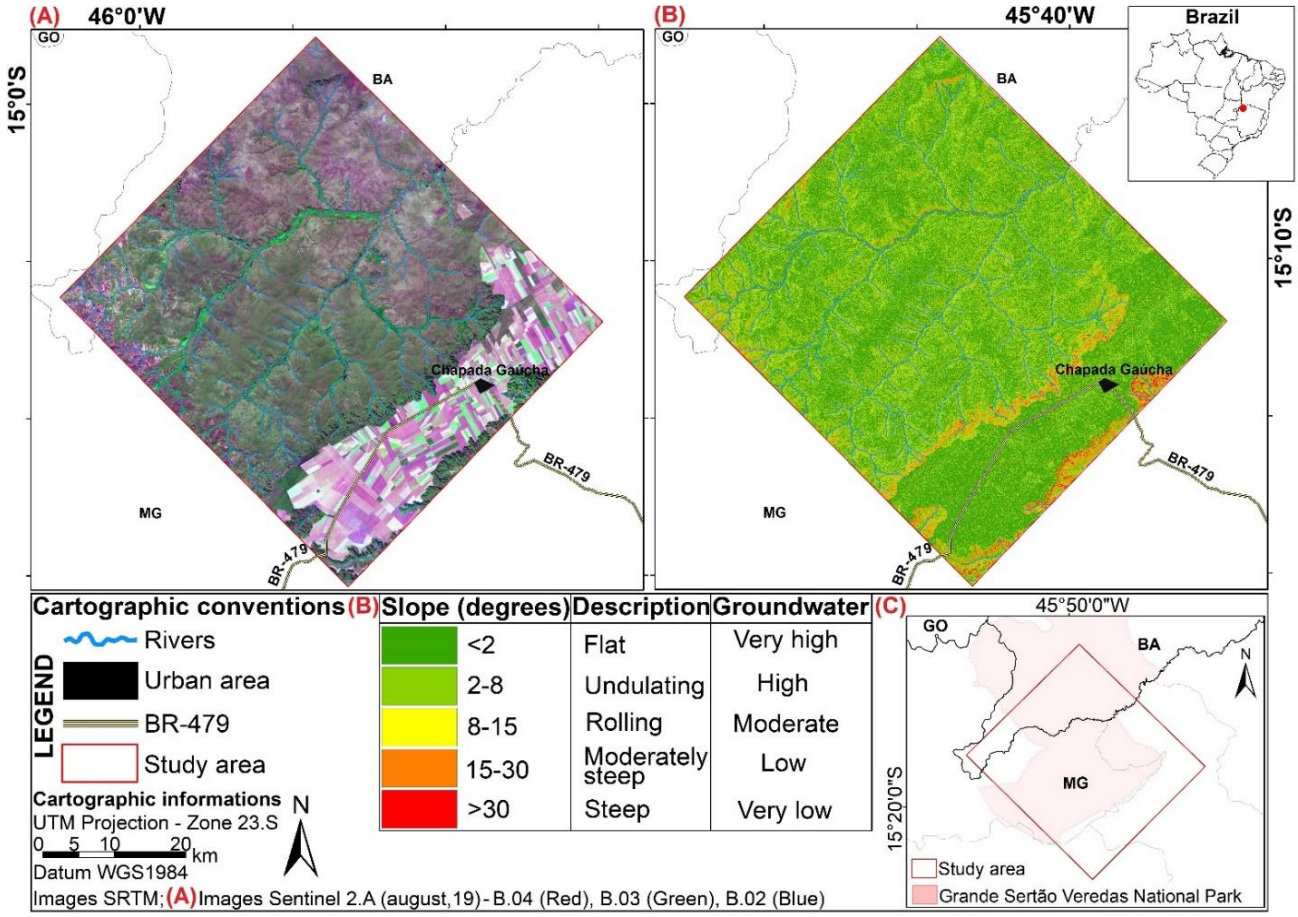

Figure 1. Location of the study area: A) MSI/Sentinel 2-A image; B) Slope map; C) Geographical situation.

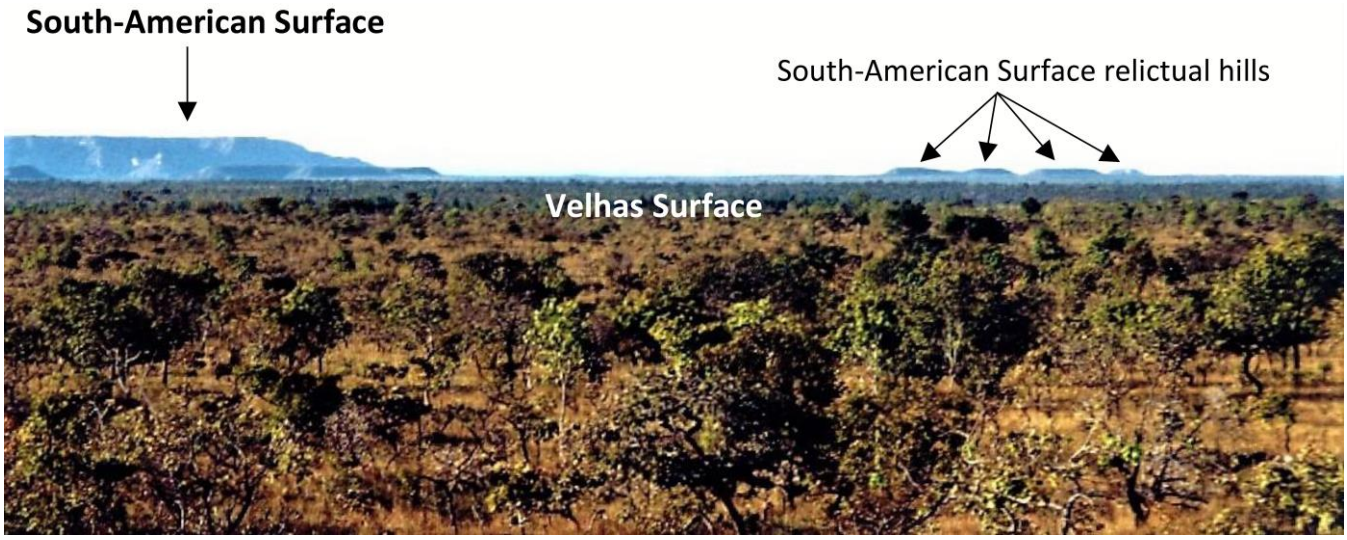

Figure 2. Landscape of the studied region (NW of Minas Gerais State) with the two levels of planation surfaces (South American and *Velhas* surfaces) recognized in the literature.

The studied region is located on the transition zone between the Cerrado and the Caatinga domains (MMA; IBAMA; FUNATURA, 2002). The regional climate marks the transition from semi-humid to the semi-arid tropical regime, with 4-6 months of drought (NIMER, 1989). The annual averages of rain and temperature (1989-1999) are 1397,6 mm and 24.4 °C (INMET, 2012). The rain season extends from November to March.

3. Method

The proposed method is based on the unsupervised classification of the frequency of elevation values for each pixel of an area. It considers that high pixel frequencies (peaks on the graph) indicate planation surfaces remnants and that the segments with low pixel frequencies (altimetrically below a peak or between peaks) are associated to the dissected reliefs of the planation surface located immediately above. So, in the proposed method, every pixel is necessarily attributed to some planation surface, belonging either to the preserved parts of this surface or to its dissected parts (Figure 3).

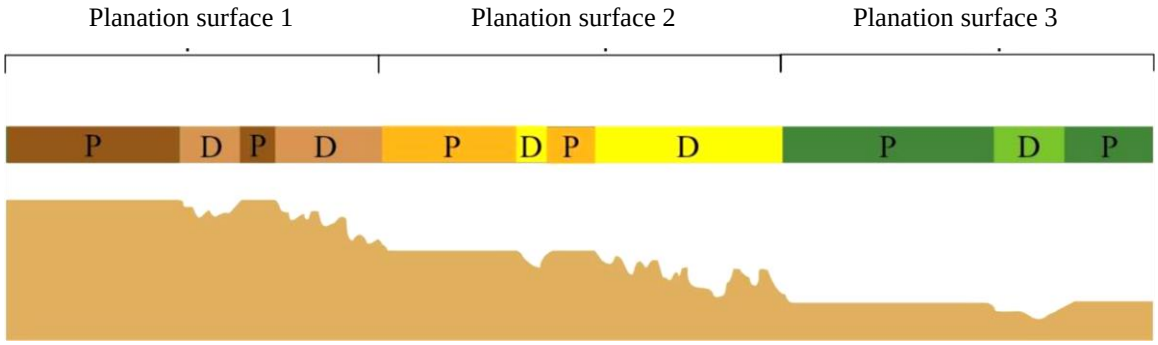

Figure 3. Hypothetical model for planation surface identification on a landscape of stepped surfaces. Each part of the landscape is considered as associated to some planation surface, belonging either to its preserved areas (P) or to its dissected areas (D).

3.1 Data Analysis Techniques

The methodological procedures were developed according to the steps presented in the flowchart of Figure 4. They were performed using images, from digital elevation model using SRTM data available on the website of ASF (Alaska Satellite Facility), resampled (up sampled) to 30 m for 12.5 m pixel size with orthometric altitude (EGM96 geoid model), converted to geometrical altitude (ellipsoidal). Secondary data from cartographic bases in shapefile format related to roads, drainage network and other cartographic elements were used, including the municipalities and states that cover the study area (IBGE, 2010). Data related to soils from RADAMBRASIL SD-23-Brasília (BRASIL, 1977) and geology acquired from the Geodiversity maps of Minas Gerais and Bahia states (CPRM, 2010), with a publication scale of 1:800.000, were also used.

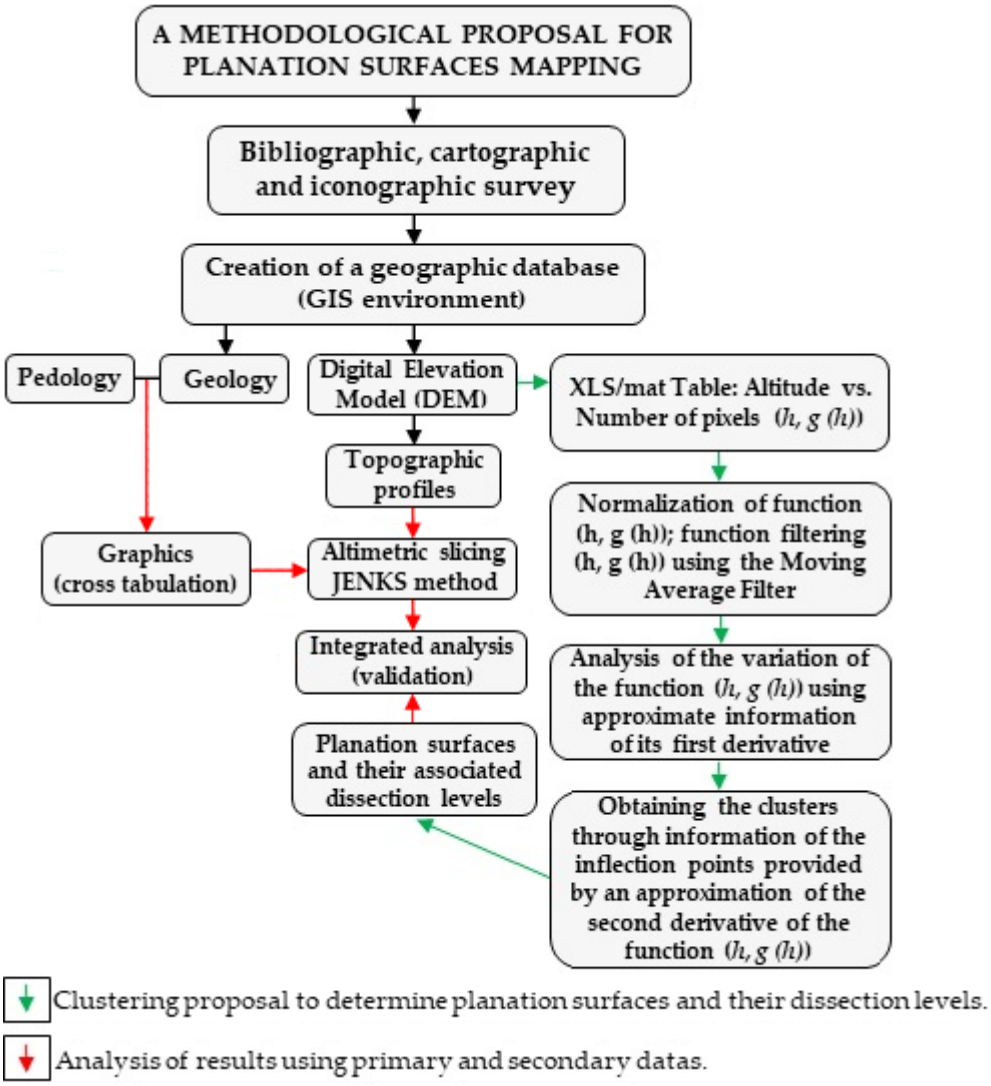

Figure 4. Flowchart illustrating the methodology.

The set of information and data used was organized in a geographic database for treatment, conversion, processing and analysis, and implemented in a GIS. The proposed publication scale of the maps was 1:360.000.

3.2 DEM treatment

A mosaic was built with the scenes from the SRTM sensor, and a security margin to delimit the study area was established. The "Fill-Sinks" algorithm was used to fill spurious depressions, assigning new values to pixels with anomalies, based on information from the closest neighbors (WANG and LIU, 2006).

The generated DEM mosaic consists of 2 columns (altitude/pixel) with 214 lines. The elevation ranged from 685 to 898 m, with an average of 783 m. Subsequently the table of attributes with the information of altitude vs. pixel was exported in an "xlsx" file (EXCEL), to be converted to a "MAT" file for reading in the MatLab software (MATrix LABoratory).

3.3 Altimetric stratification and planation surfaces identification

The spatial distribution data of the altitude by number of pixels provides a non-linear function represented as a function of number of pixels vs. altitude h (H is the set formed by the different values of altitudes of the study area), $g(h)$, as shown in figure 5.a. It was adopted as hypothesis that each inflection point of this function, altitude vs. number of pixels, represents a geometric signature for altimetric stratification providing, however, no information about the spatial distribution of the strata. Higher frequencies of altitude pixels indicate possible planation surfaces.

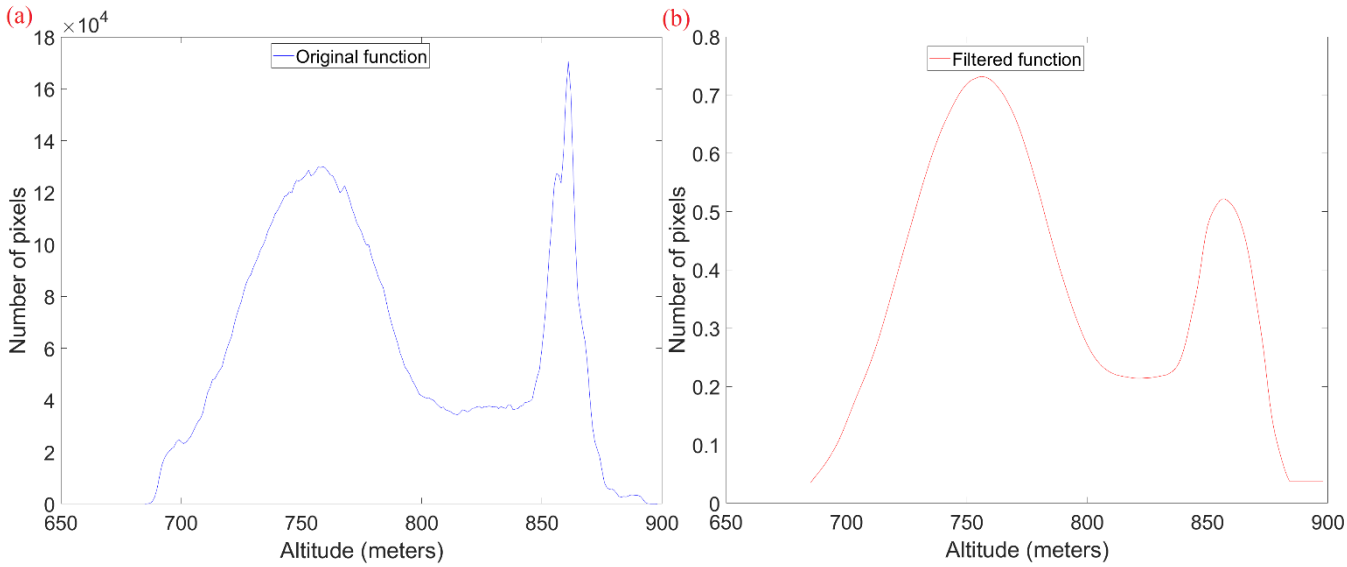

Figure 5. Graph of altitude *vs*. number pixels (a) Real values of frequency; b) Filtered and normalized values of frequency

The proposed clustering technique was based on digital treatment of the image signal and the study of the variation of $g(h)$ function. The digital treatment consists of filtering the signal using MatLab's "Moving-Average" filter to eliminate minor irrelevant variations or acquisition noise (Figure 5.b). The study of the variation of the function g (h) was carried out using a technique of analysis of the change in the concavity, inflection points, of this filtered and normalized non-linear function, based on the variation of the function given by the sign of the first derivative (Equation 1) and Propositions 1 and 2. In this analysis, adopting a pre-established reference $(H_0, g(H_0))$, local inflection points are evaluated using information from the second derivative signal (Proposition 3) (LEITHOLD, 1989).

Proposition 1 provides a criterion for determining the intervals where a function is increasing (a), the intervals where it is decreasing (b), and, where it is constant (c).

Proposition 1: Let $f(x)$ a continuous function in an I interval, and differentiable within it. If, for every point x interior to I, it is verified:

(a) $f'(x) > 0$, then $f(x)$ is growing in I;

(b) $f'(x) < 0$, then $f(x)$ is decreasing in I;

(c) $f'(x) = 0$, then $f(x)$ is constant in I.

Propositions 2 and 3 provide criteria for determining the nature of a point c in the domain of function f, which can be a maximum, minimum or an inflection point (LEITHOLD, 1989).

Proposition 2: Let f be a continuous function in the interval $[a, b]$ and derivable in the open range (a, b), then there is c such that:

$$f'(c) = \frac{f(b) - f(a)}{b - a}$$

Proposition 3: Let c be a point in the domain of a function f, such that its first derivative, $f'(x) = 0$. Then,

(a) If $f''(x) > 0$, that is, the second derivative of f in c is greater than zero, so c is the local minimum point of f;

(b) If $f''(x) < 0$, , that is, the second derivative of f in c is less than zero, so c is the local maximum point of f;

(c) If $f''(x) = 0$, , the second derivative of f is zero in c, then c is an inflection point.

The proposed algorithm to group the initial surfaces is built using the implicitly derivatives concept, and consists of analyzing the variation of function of number of pixels, $g(h)$, by altitude, (h). Thus, based on proposition 2, relative metrics are used to obtain a function, d(h), which is obtained by calculating the distance between the points of secant lines defined by the size of a pre-established window, W, and the function $g(h)$.

The direct calculation of the first derivative using the definition of derivative (Equation 1) to obtain the initial grouping is not adequate, considering the database as it was obtained, because even with the signal filtering, the function $g(h)$ presents inflection points that do not characterize a group, that is, small variations occur that interfere in the value of the derivative of the function, and do not provide accurate information about their real physical behavior. Thus, the procedure for indirectly calculating the variation of the function $g(h)$, based on Proposition 2, performed through secant lines through a window W, is illustrated in Figure 6. The calculations of the secant lines between the extreme points of a window, W, were performed according to equation (1).

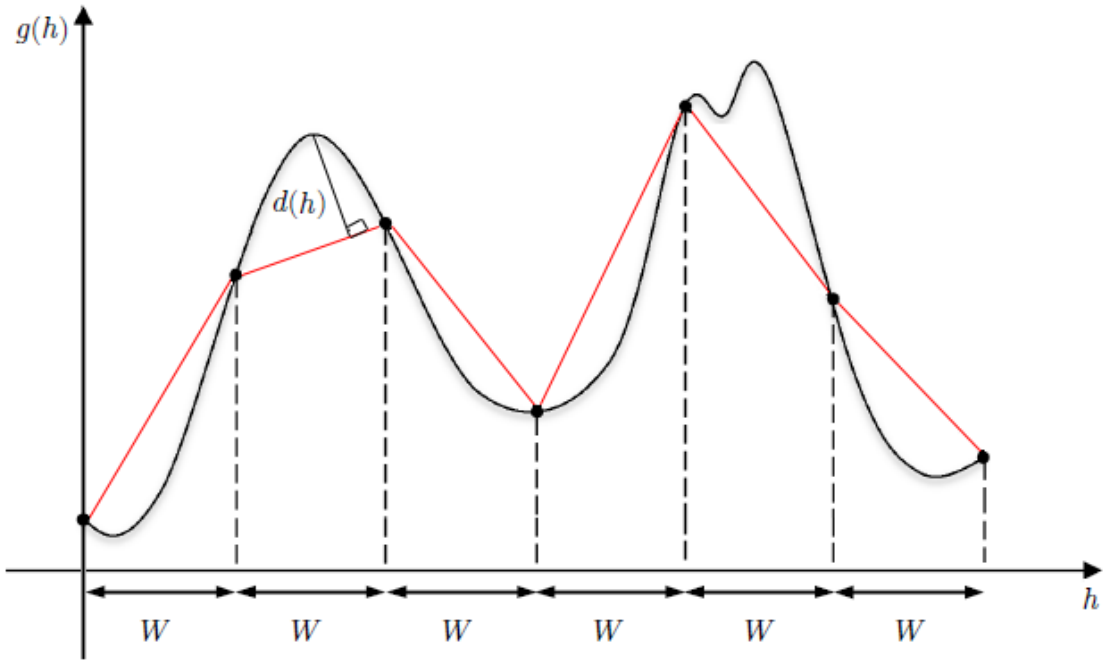

Figure 6. Determining the concavity of function by analyzing the secant line between two points in its domain.

The equation of the secant line of the function $g(h)$, of lengths equal to the length of the window, *W*, that passes through the points (X_i, Y_i) and (X_f, Y_f) is given by Equation 1.

Eq.1.

$$s(h) = CAh + k$$

CA: Angular coefficient of the tangent line, and k a constant given by the relation $k = Y_i - CAX_i$.

The orthogonal distance between a point $(h_i, g(h_i))$ situated on the function g(h) and the secant line (2), is illustrated in Figure 7.

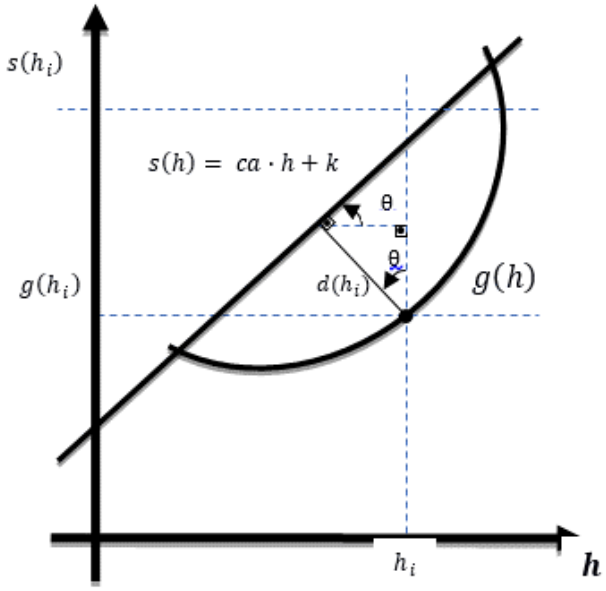

Figure 7. Geometry of calculating the distance between a point and a line.

The slope of the line in equation 2, CA, is the $tg\ \theta$ in Figure 7. The orthogonal distance $d(h_i)$ of h_i point, between the line (2) and the function $g(h_i)$ is obtained using the trigonometric relations of Figure 3, according to Equation 2.

Eq.2.

$$d(h_i) = \frac{CAh_i + k - g(h_i)}{\sqrt[2]{1 + CA^2}}$$

After the definition of the distance function $d = d(h)$, for $h \in H$, according to Equation the initial grouping is proposed (3), through the analysis of the zeros of this function throughout its domain, where the points between two zeros of the function $d(h)$ indicate changes in the concavity of *g(h)*. The function $d(h)$, illustrated in Figure 8-a, represents the approximate calculation of the first derivative of the function g(h).

The initial groups obtained through this analysis still show inaccuracies, because the technique used to determine them does not have the ability to accurately obtain the inflection points of function of number of pixels by altitude, $g(h)$. The refinement of the groups is performed using the derivative of the distance function (second derivative of the function *g(h)*), the function $d(h)$, Proposition 3, as illustrated in Figure 8-b.

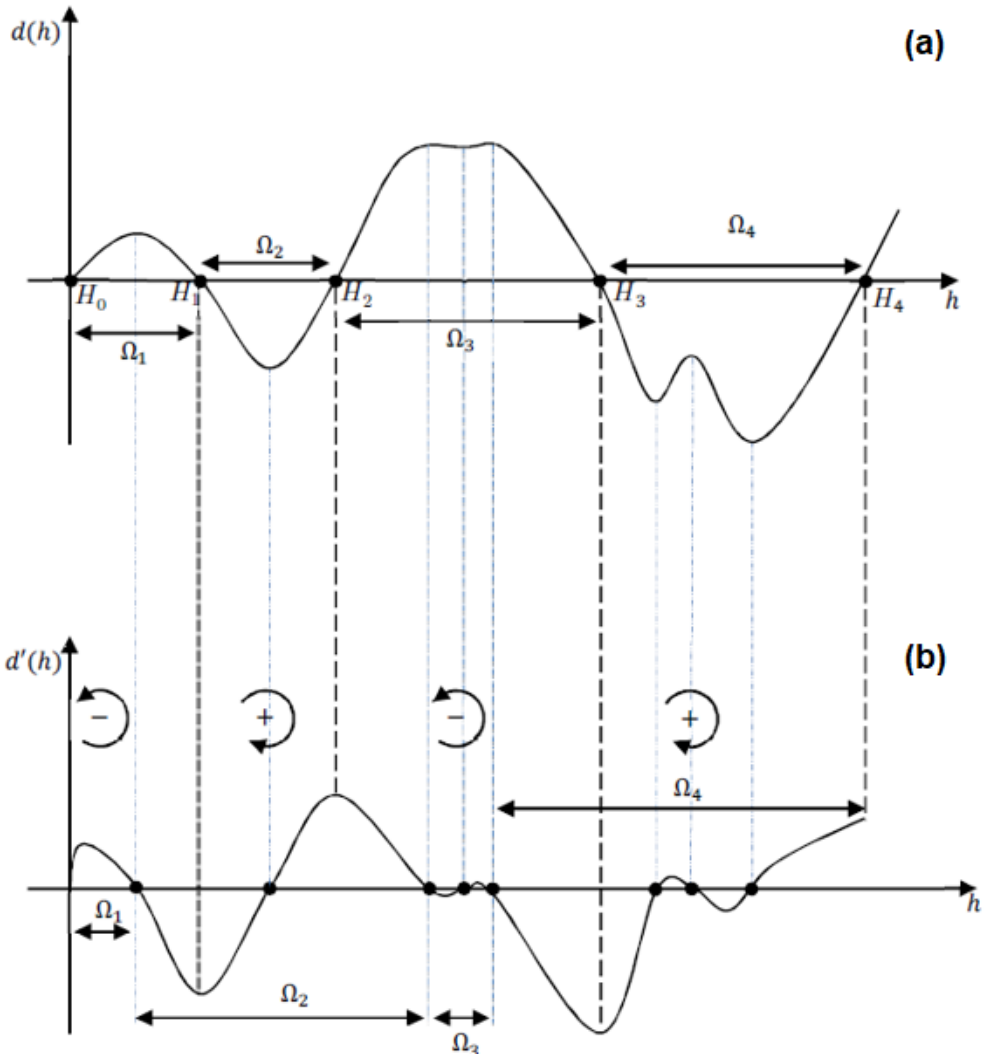

Figure 8. Illustration of the initial clustering technique and cluster refinement.

The new dimension of each of the pre-established groups A^I is refined considering the sign of derivative d'(h), and the minimum, maximum and inflection points of $d(h)$, that is, the points in the domain where d'(h)=0, which are the inflection points of function $g(h)$ (Proposition 3). In this way the predetermined size of each group A^I is redefined considering it to be composed of the set of points belonging to A^I in the interval that consists of starting point of the group A^I and ending at point H_i, where the function $d(h)$ is maximum or minimum, ie, $d'(h) = 0$. Therefore, the first and second derivatives are calculated in an approximate way, to avoid taking slopes that are not configured like groups. The clustering algorithm proposed in this paper is detailed below.

3.4 Grouping algorithm

The main steps for applying the clustering algorithm are described below:

1. Reading the database of the study area: Table (xlsx) of altitude vs. number of pixels. This database makes up the original function with several acquisition noises;
2. Setting the window size parameter, W, concerning the database;
3. Normalization of the function altitude by number of pixels, and filtering using the moving average filter to eliminate small variations in measurement and signal acquisition, obtaining the function $g(h)$. In the filtering of this function, there is a shift in the abscissa axis equal to half from the window $\left(\frac{W}{2}\right)$, between the function originally defined by the database and the filtered function. This shift in the value of altitudes is eliminated in this step and the functions, original and filtered, are put in phase.

Eq. 3.

$$g(h) = d_d\left(h + \frac{w}{2}\right)$$

4. Putting, the filtered signal function $g(h)$ at the same altitude reference as the original function (Equation 3);
5. Determining, the functions $d_1(h)$ e $d_2(h)$ (Equation 2), dividing the function curve $g(h)$ in length segments of the same size as the W window, to obtain the function $d_1(h)$, and half the size of the window $\left(\frac{W}{2}\right)$, to get the function $d_2(h)$;
6. Obtaining the function $d(h) = d_1(h) + d_2(h)$. This function d(h)represents indirectly the first derivative of $g(h)$, and allows to numerically determine the concavity of the function $g(h)$;
7. Performing, the initial grouping A_i^I, scanning the function $d(h)$, as shown in Figure 8.a. From the starting point H_0 of the domain of $d(h)$, a scan is made in the increasing direction of the domain of $d(h)$ until it finds its first zero, the point H_1, then defining the first group A_1^I , formed by the altitudes that comprise the $\Omega_1 = [H_0, H_1]$ interval. The second group is obtained from H_1 until it finds the next zero of $d(h)$, the point H_2, defining the second group A_2^I with altitudes that comprise the interval $\Omega_2 = [H_1, H_2]$. This procedure is carried out until you find the last valid altitude value and thus obtain the last group (Figure 8.a). The set of initial groups can be defined as:

Eq.4.

$$A^I = \{A_i^I | h_i \in \Omega_i \text{ ^} d(H_i) = 0, \qquad i = 1, NG\}$$

NG: Number of groups obtained by analyzing the function.

8. Performing, fine adjustment of the initial cluster intervals:
   - Obtaining the function equivalent to that derived from the function $d(h)$ of determine the points in its domain where it is maximum and its inflection points (sign change). The groups are defined by the sets of heights, h, between two inflection points of $g(h)$.
   - In the first group, A_1^I, from H_0, determine the first point of zero, H_1', of function $d'(h)$, which is the value where $d(h)$ is maximum (or minimum). From H_1', continue scanning in the domain of $d'(h)$ until finding a maximum (or minimum) point, which corresponds to the limit of group A_1^I. The new group is then redefined as being with the new interval $\Omega_1 = [H_0, H_1']$. In the case where $d(h) > 0$, an adjustment occurs by reducing the interval Ω_1, and the domain points between H_1' and H_1 become part of the group A_2. Proceeding with the adjustment procedure, the next group is determined considering which $d(h) > 0$, and the point where your maximum, $d'(H_2') = 0$ occurs. The A_2 group is redefined as the altitudes that belong to the $\Omega_2 = [H_1', H_2']$ set. In the case of group A_i^I, where $d(h) < 0$, an adjustment of the interval occurs by increasing its number of points. In Figure 8.b, this procedure is illustrated. In general, the final grouping is given by the following criterion:

Eq. 5.

$$A_i = \{A_i^I | h_i \in \Omega_i \; and \; d'(H_i) = 0\}$$

where:

$$\Omega_i = \{H_i | H_i < H_j \;\; if \;\; d(H_j) > 0 \;\; or \;\; H_i > H_j \;\; if \;\; d(H_j) > \; 0 \; and \; H_j \in H_i \}$$

The results obtained by the algorithm proposed in this study were compared to the results obtained through the natural breaks algorithm (JENKS), using elevation data from the same study area. For this, the same number of classes provided by the algorithm proposed in this study was adopted. The spatial distribution of the altimetric intervals of the DEMs was analysed and the frequency histograms were graphically presented in order to verify the distribution of the spectral behaviour.

4. Results and discussion

The only parameter required to be calibrated in the proposed algorithm is the size of "W" window (measurement unit in meters). For the adopted control area, where there is reliable knowledge of the planation clusters, it was found that the window size for the algorithm to obtain good precision for classifying the groups is $W = 27$ meters. The algorithm was implemented in the MatLab software (MATrix LABoratory), using all its implicit functions.

4.1. Planation surfaces

The graph in Figure 9 shows the results of the clusters determined by the proposed algorithm.

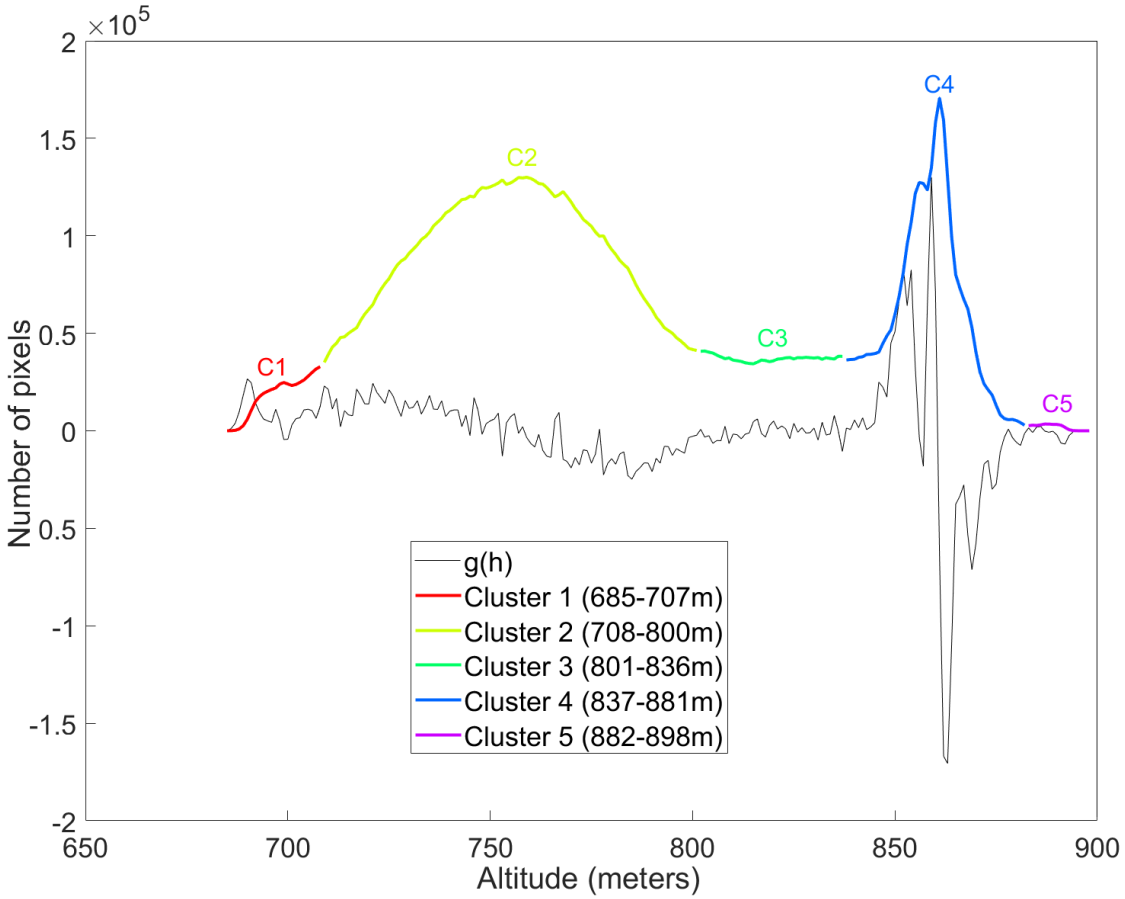

Figure 9. Results provided by the proposed algorithm for the control area.

As shown in the graph in Figure 9, the "C2" and "C4" clusters correspond to highest frequency peaks. However, the spatial configuration of both is different. The "C2" cluster has a wider range of altitude than the "C4" cluster, indicating that there are more pixels varying as a function of altitude in "C2". This does not mean that, as there is greater variation in altitude, the spatial coverage is greater. This indicates that this is a surface with a lower degree of flattening and/or with a regional slope (unlevel surface). Consequently, the degree of flattening/leveling of "C2" is lower than the degree of flattening/leveling of "C4". The "C1", "C3" and "C5" clusters represent the change in the concavity of the function, using the signal information of the first derivative, where it is verified that the function g (h) presents a smoother behavior for these altitudes, that is, it presents a variation in the number of pixels in different altitude ranges. These clusters are associated with the dissected reliefs of the planation surfaces.

Based on the results of the graph in Figure 9, the clustering methodology delimited the area in 5 clusters, comprising the following altimetric intervals: Cluster 1: 685-707 m; Cluster 2: 708-800 m; Cluster 3: 801-836 m; Cluster 4: 837-881 m, Cluster 5: 882-897 m (Figure 10).

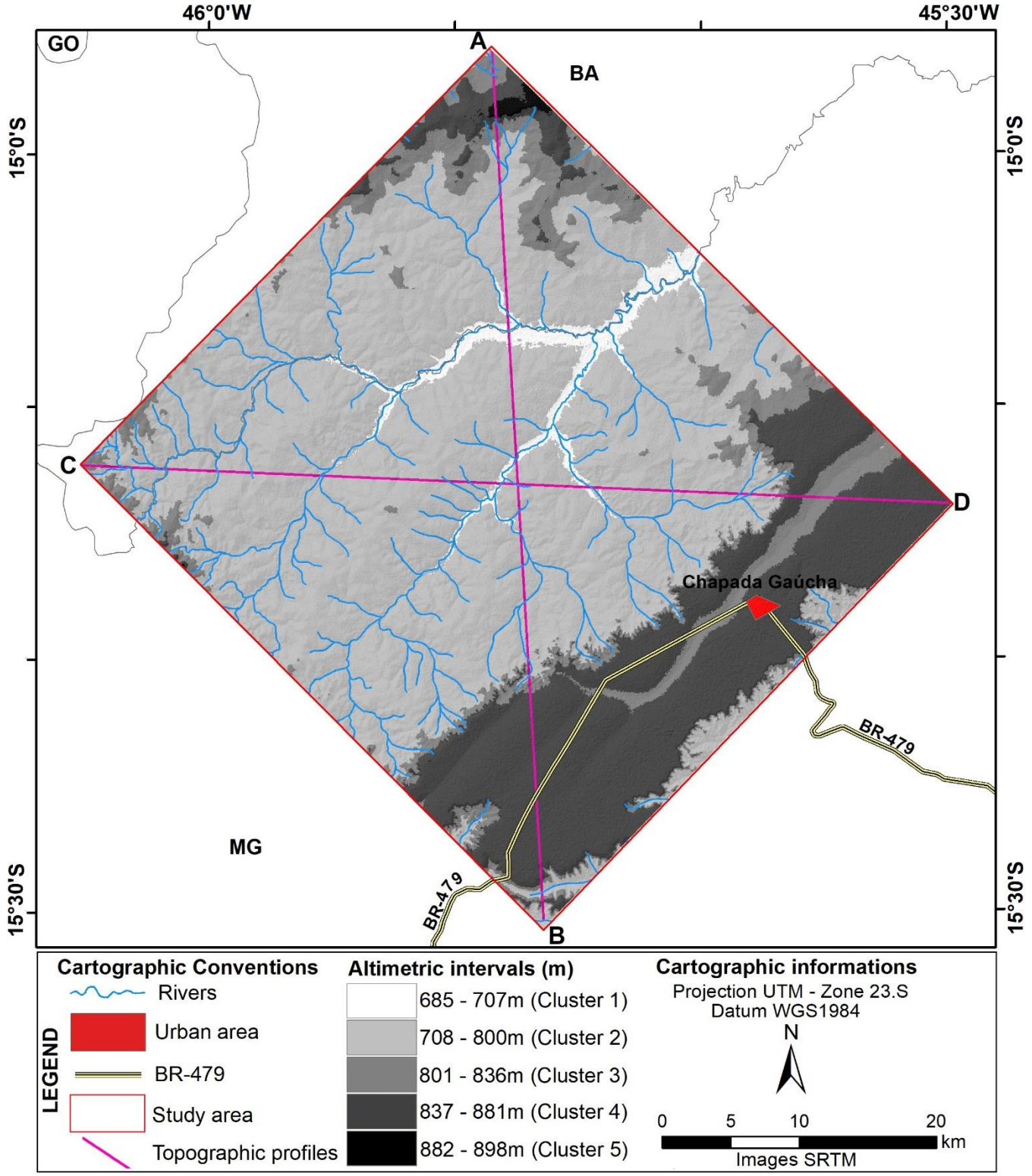

Figure 10. Altimetric slicing of the area based on groups (clusters) provided by algorithm.

After identifying the groups and extracting the altitude values for each identified planation surface, the altimetric intervals between them were considered dissected areas. These intervals were considered as previously belonging to the planation surface immediately above. Thus, the intervals were reclassified for quantification and elaboration of a map, in order to verify the spatial distribution of the flat tops, identified as remnants of the planation surfaces. For example: "Cluster 1" was considered a dissected area and Cluster 2 as a flat remaining area of the same planation surface (Surface 3) (Figure 13). Cluster 3 was considered as a dissected area and "Cluster 4"

as a flat remaining area of the Planation Surface 2. Finally, Cluster 5 was considered as a dissected area of Surface 1; no flat remnants of this surface were identified in the studied area.

The Figure 11 illustrated the North-South and East-West topographic profiles, with the reconstitution of the proposed surfaces, encompassing all the compartments mapped for the study area.

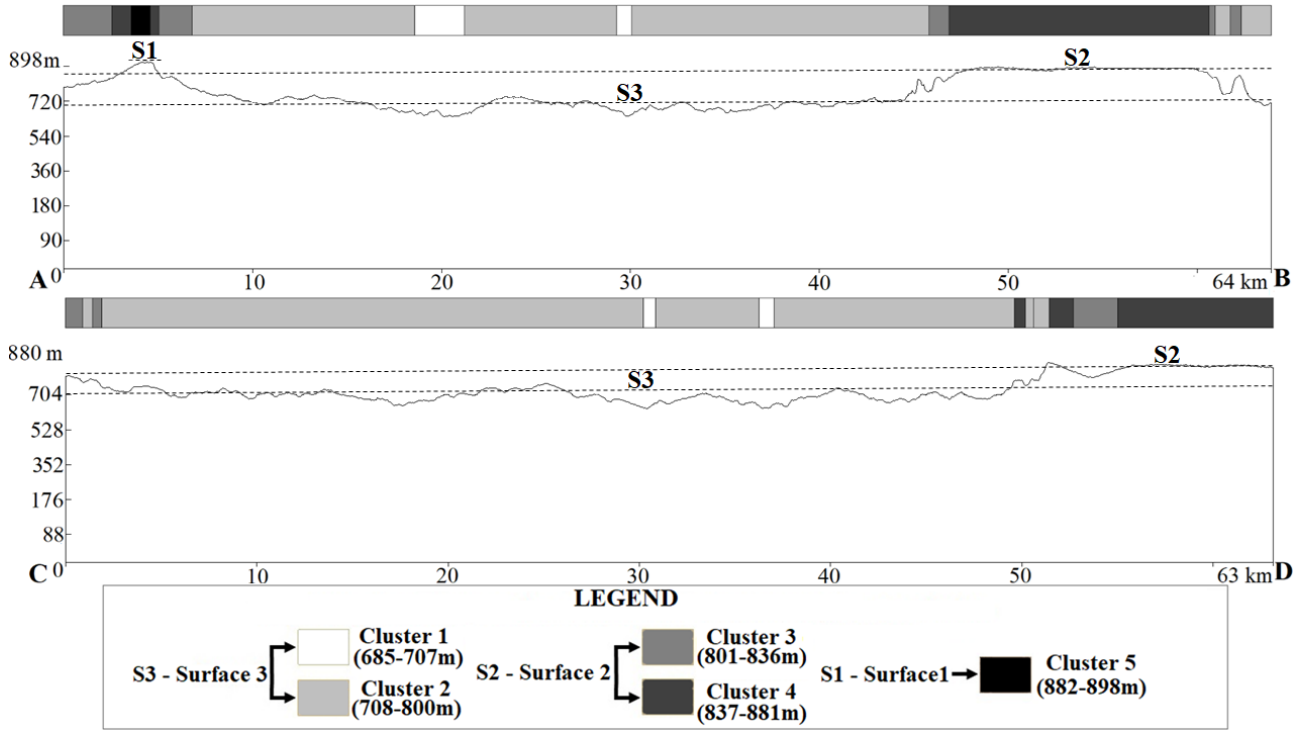

Figure 11. Topographic profiles (A-B); (C-D).

In profile A-B, that shows the three mapped surfaces; the surface 3, the lowest one, is located between 685 and 800m; the Surface 2, intermediate in altitude, corresponds to the *chapada* area, between 801 and 881m; the surface 1, the highest one, located, between 882 and 898m. In profile C-D, only the Surfaces 3 and 2 are presented. The photograph of Figure 12 was taken facing North, from the edge of the *chapada* (Surface 2). It shows the lowlands of Surface 3 with relictual hills of Surface 2.

Thus, the model allowed to associate the landforms *pixels* of the area to three planation surfaces, the highest being Surface 1 and the lowest being Surface 3 (Figure 12).

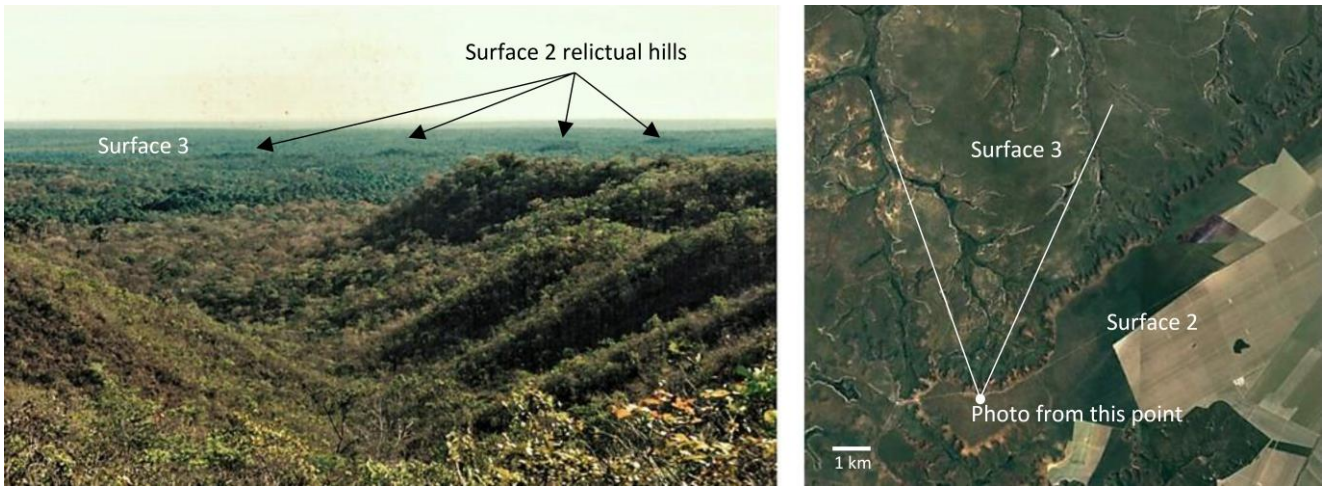

Figure 12. Left: photography from the edge of the *chapada* (Surface 2) showing the lowlands of Surface 3 with relictual hills of Surface 2. Right: location of the point from which the photograph was taken in the context of the two planation surfaces.

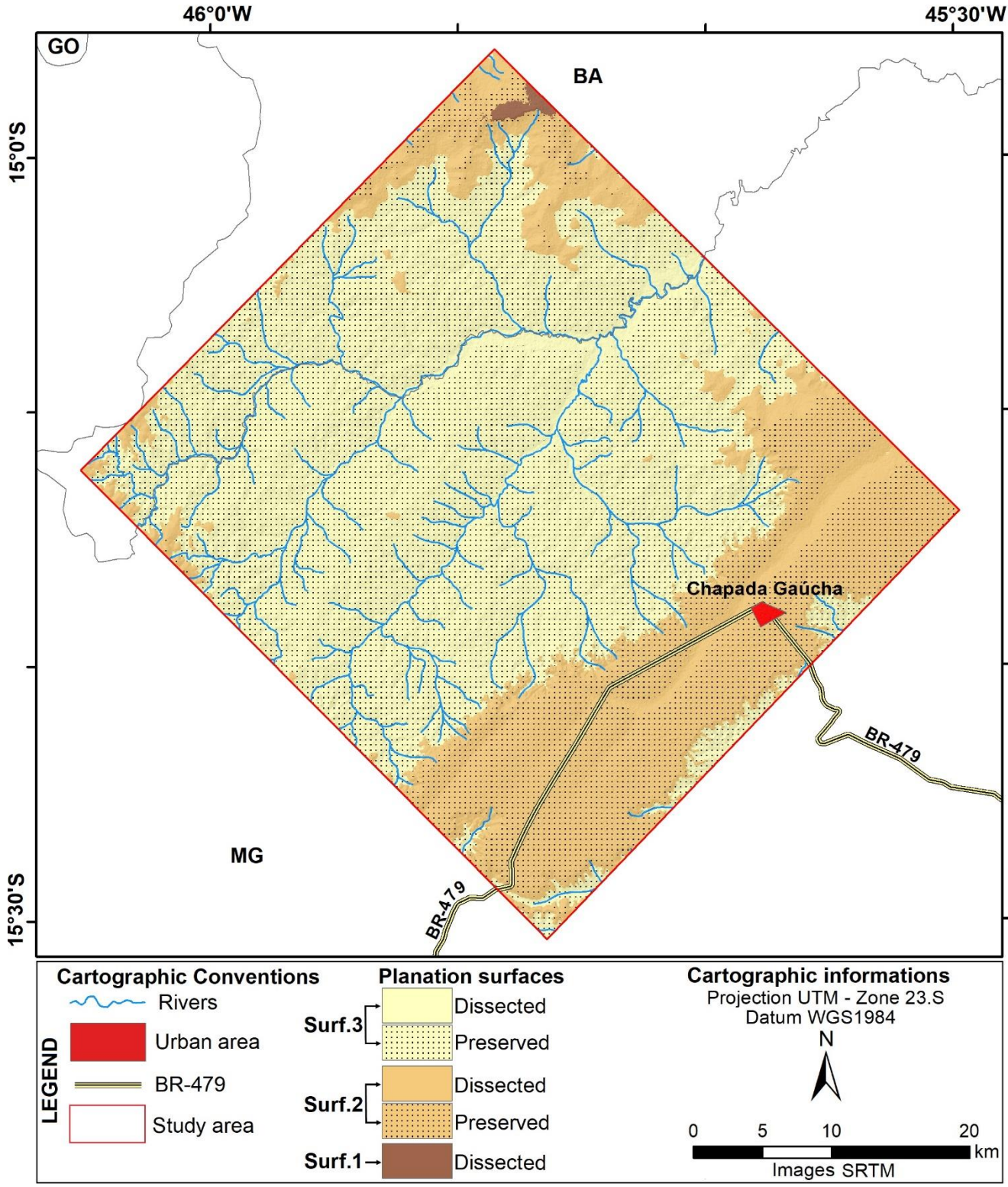

Figure 13. Map of planation surfaces, composed of flat remnant areas, and their respective dissected levels.

Planation Surface 3 corresponds to the lowest level, being the group formed by cluster 1 (dissected), represented by the hidromorphic or incised valleys and floodplains, with slopes less than or equal to 3%, and cluster 2 (preserved), where the relief presents interfluves with flat or gently convex hill tops with slopes less than 8%. This planation surface can be related to King's (1956) *Velhas* Surface or to the South American I Surface of Valadão (2009). Although the flat areas are not dominant in the preserved parts of *Velhas* surface, this

subcompartment is indicated by the pixel concentration (cluster 2) on the graph of Figure 9 and by the relative accordance of its summits (excluding the summits of relictual hills and *mesas* of Surface 2, Figure 13). The broadness of C2 cluster peak (Figure 9) is explained by the low degree of planation and by the unlevel of *Velhas* Surface in the studied area, which gently slopes northwards. In fact, *Velhas* Surface is described in the literature as an undulating surface (AUGUSTIN et al., 2009; VALADÃO, 2009) which is, also, oriented towards the regional base-level, the *São Francisco* river (VALADÃO, 2009). The dissected parts of this surface comprise mainly flat-bottomed swamp valleys (*veredas*), which are formed by geochemical incision (LIMA; QUEIROZ NETO, 1996; MELO, 2008).

Planation Surface 2 is the set of clusters 3 and 4. This planation surface can be related to the South American surface of King (1956) and of Valadão (2009). The cluster 3 is the dissected part of this surface, located at the edges (escarpments) of the plateau (*chapada*) level, with slopes from 9% (undulating relief) to 41% (strongly undulating). In addition to the plateau edges, inside the flat (preserved) part of this surface there are also dissected areas, associated to an open and large river channel. Cluster 4 refers to the preserved reliefs of Surface 2 (*chapada*). It differs from Surface 3 in that it has a higher degree of flattening, as indicated by the sharpness of the cluster "C4" peak when compared to that of the cluster "C2" peak (Figure 9). This is in accordance with the literature, which highlights the exceptional degree of topographic leveling of the South American Surface (BRAUN, 1970; VALADÃO, 2009). The Surface 2 preserved areas are, therefore, much flatter than the preserved areas of Surface 3. This would not be expected – as Surface 2 is older than Surface 3 – but can be explained by the longer time of elaboration of Surface 2 and by the presence of mature duricrusts covering and protecting this surface from erosion (BRAUN, 1970; COSTA, 1991; VASCONCELOS et al., 1994; VALADÃO, 2009).

Cluster 5 was interpreted as representing the remnants of the highest surface of the study area (Surface 1). It comprises only dissected landforms, with no flat tops. It is restricted to small areas of the northern portion of the study area. These landforms were here attributed to the Post-Gondwana surface proposed by King (1956). Remnants of planation levels older than South American Surface, standing out from this surface, are described by Braun (1970) and Lanza; Ladeira (2013), for the central part of Brazil.

The results of the proposed algorithm were compared to the results from JENKS method. This method was processed classifying the number of cluster in 5, to follow the same pattern for the algorithm here proposed (Figure 14).

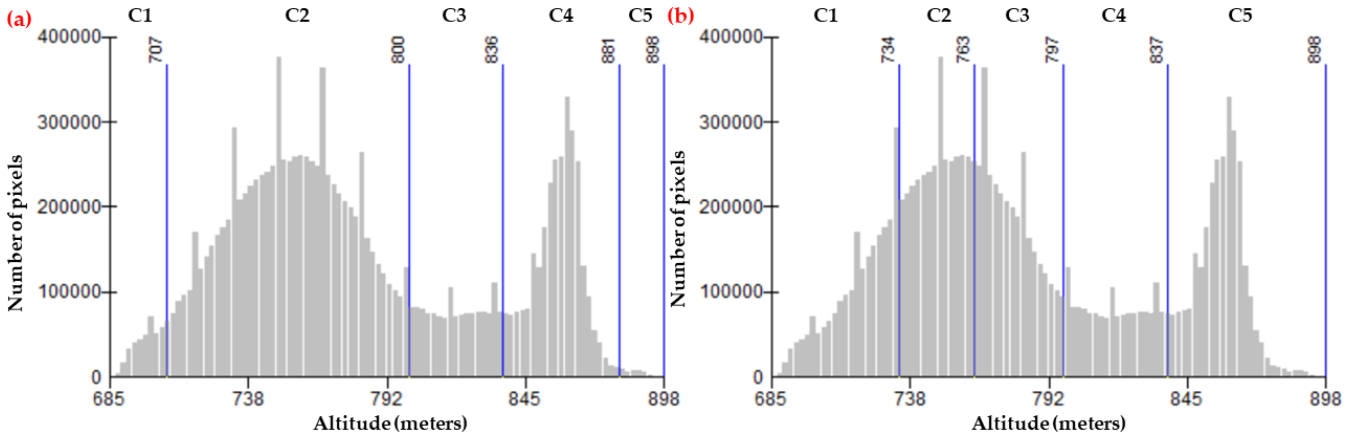

Figure 14. Histogram stratification: a) provided by the proposed algorithm; b) provided by JENKS.

It can be seen in Figure 14 (a) that the proposed algorithm demarcated the boundary between Surfaces S1 and S2 (clusters C5 and C4), unlike JENKS method, which considers this range of pixels as just one surface. For S3 Surface, where the proposed algorithm identifies the broad peak and distinguishes clusters "C1" and "C2", the JENKS method divides this extensive pixel frequency range into three clusters "C1", "C2" and "C3", what is not

suitable to the purpose of identification of planation surfaces. Thus, only cluster "C4" for JENKS method showed some correspondence with a cluster identified by the proposed algorithm (C3), indicating the dissected areas of S2 Surface. Thus, analysing the results provided by the JENKS for the studied area, it appears that the classification was not suitable for the geomorphological purpose of planation surface identification on the studied area.

4.2 Relationship between planation surfaces and soil types

A noteworthy correlation was observed between the mapped planation surfaces and the soil types found in the studied area (Figure 15 and the graph of Figure 16):

- Planation Surface 3 is covered, in its subcompartment of dissected relief, by Gleysols in more than 90% of its area and by Ferralsols in only 6% of its area. The presence of Gleysols is explained by the fact that they are located on hydromorphic valleys, which mark the initial stages of geochemical incision of this planation surface (LIMA and QUEIROZ NETO, 1996; MELO, 2008). In its preserved subcompartment, more than 70% of the area is covered by Arenosols, followed by the Gleysols (13%), Cambisols (8%) and Ferralsols (3%). The Arenosols dominate, therefore, the flat or convex interfluves part of this planation surface and may result either from the pedogenesis of sandy materials deposited as a result of retreat of the *chapada* escarpments, or from a pedogenesis in a past environment of less efficient internal drainage, resulting in xanthization and clay impoverishment (PETERSCHMITT et al., 1997).

- Planation Surface 2 presents, in its dissected subcompartment, the undulating to strongly undulating reliefs (Figure 1. (B)) associated to the edges of the plateau. The main soil types are Arenosols (48%), Ferralsols (30%) and Cambisols (22%). The Arenosols were interpreted as parts of the Planation Surface 3 that were mistakenly included in the dissected subcompartment of the Planation Surface 2, while the Ferralsols would correspond to parts of the flat (preserved) subcompartment of Planation Surface 2, also erroneously included there. Inaccuracies in the method proposed here and, above all, the scale incompatibility between the proposed surface map and the soil map available for the region, would explain the inconsistencies observed for this narrow band shaped subcompartment. Therefore, considering the landforms and the slope of the plateau edges (Figure 1. (B)), it is believed that the dominant soil type in this subcompartment is the Cambisol. A field-work or major scale soil maps would allow testing this hypothesis.

The flat subcompartment of Planation Surface 2 presents essentially Ferralsols (89%), with 6% of Arenosols and 5% of Cambisols. The elevated position in relation to the surrounding reliefs, favoring the internal drainage of soils, as well as the long period of elaboration of this planation surface (South American) (VALADÃO, 2009), would have been responsible for the formation of the thick Ferralsols mantles.

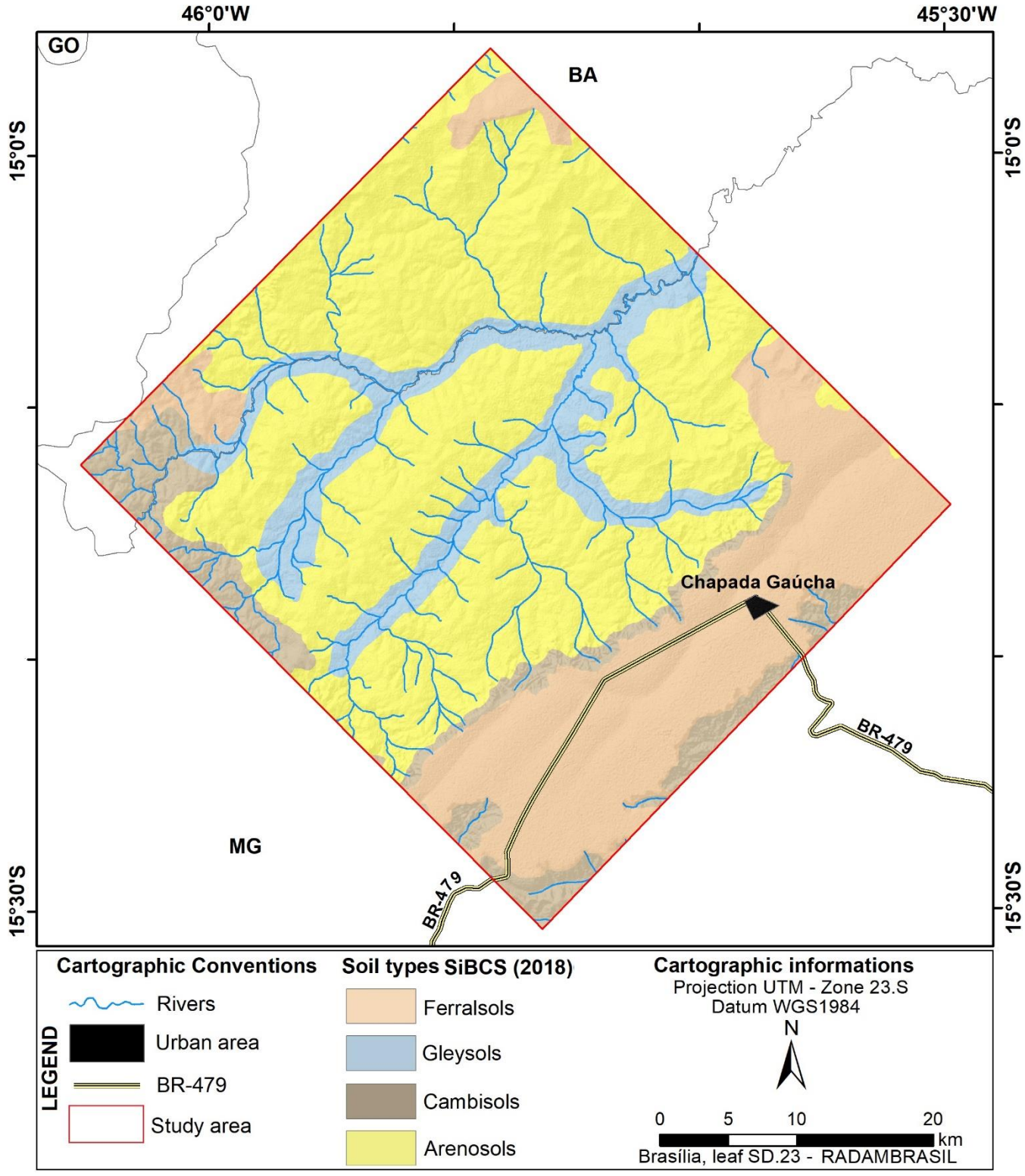

Figure 15. Soil map (RADAMBRASIL (SD-23-Brasília).

- Planation Surface 1 is represented only by its dissected subcompartment. Ferralsols are the dominant soils, occupying 99% of the surface. The presence of Ferralsols can be attributed to the absence of steep slopes and the long exposure of materials to weathering and pedogenesis.

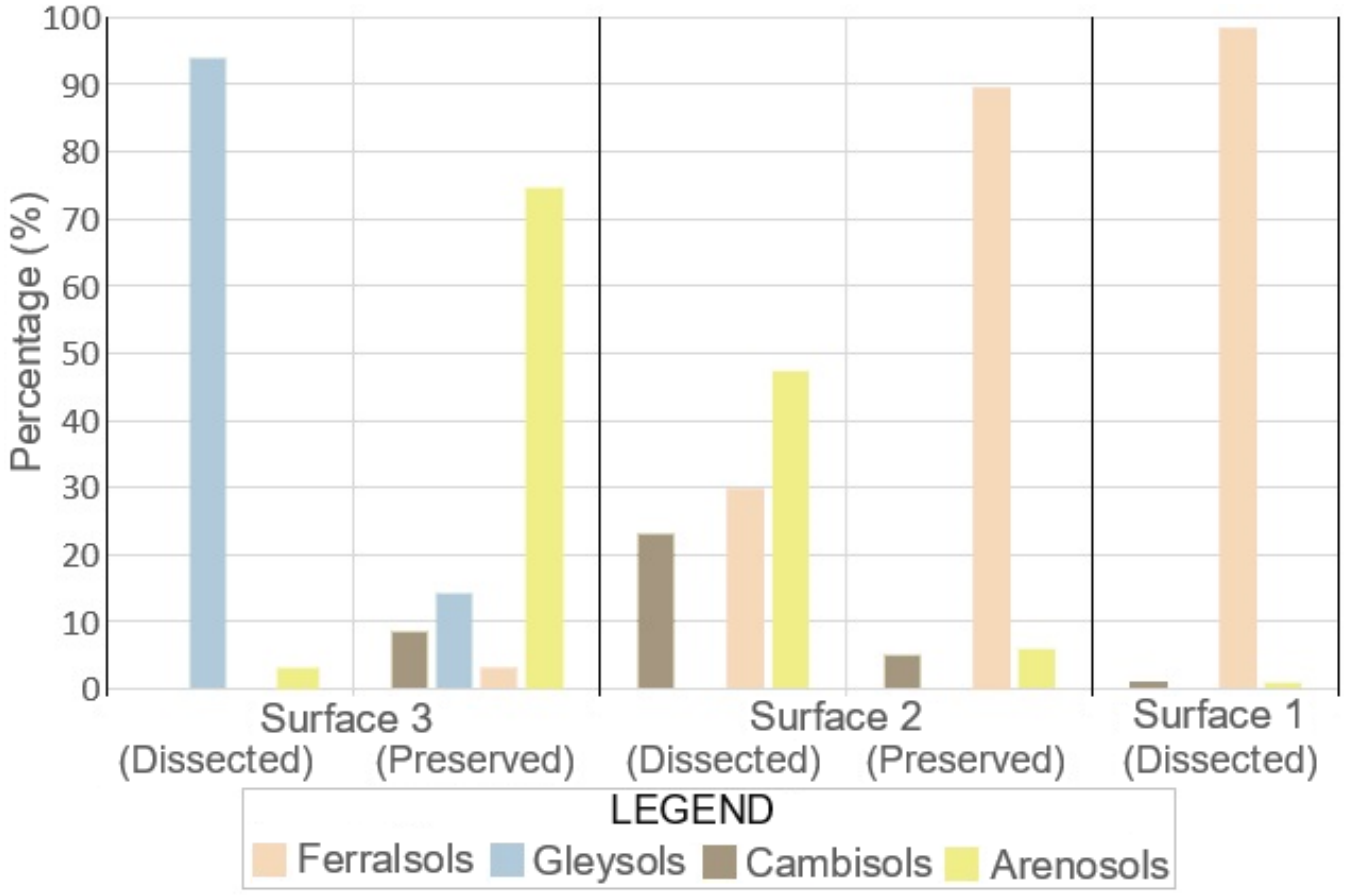

Figure 16. Graph of distribution of soil types on the planation surfaces (preserved and dissected).

4.3 Relationship between planation surfaces and geologic units

Figure 17 shows the distribution of the geological units in the studied area and Figure 18 shows the percentage of each geologic unit for each planation surface. The Figure 17 indicates that the dominant geologic unit for all surfaces, except for the preserved area of Surface 2 and the dissected area of Surface 3, is the Urucuia Group. If we consider that the geological unit of Lateritic covers with iron duricrusts (which dominates the preserved area of Surface 2), and that the geological unit of Alluvial deposits (which dominates the dissected area of Surface 3) are, in fact, *in situ* surficial formations, all surfaces might have the Urucuia Group sandstones as the main substrate, except for the small areas on the Areado Group and on the Três Marias Formation. The Alluvial deposits unit are, in fact, mainly hydromorphic soils (Gleysols), associated to the poorly drained *vereda* valleys, elaborated by the geochemical incision of Surface 3.

Therefore, it appears that the lithological control was of secondary significance for the configuration of planation surfaces in this area, as all the three surfaces have the sandstones of Urucuia Group as the main substrate. No information was obtained on the geologic structure for this mapping scale. This would allow assessing the influence of structural control for the development of planation surfaces or drainage network.

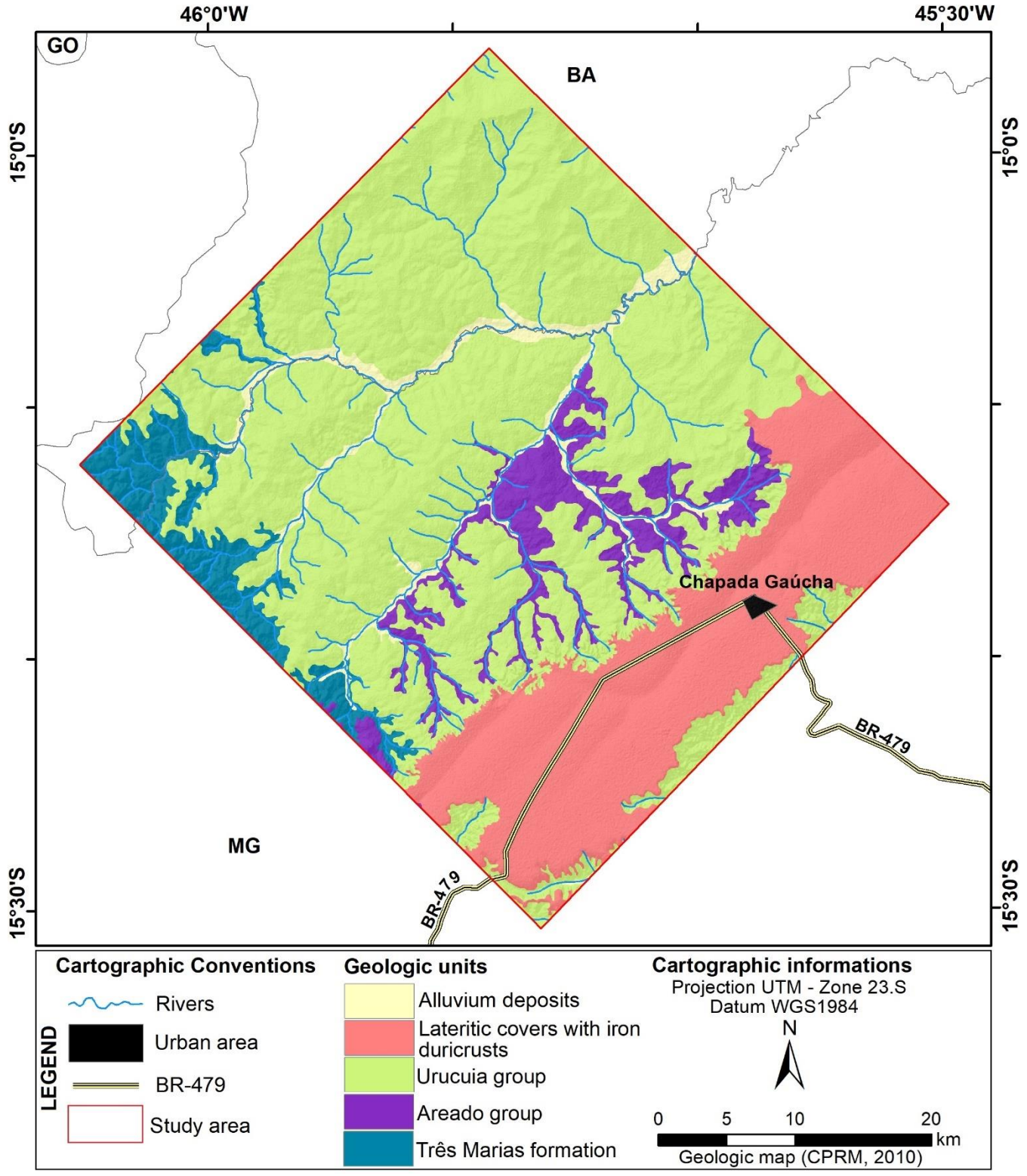

Figure 17. Adapted from Geologic map (CPRM, 2010).

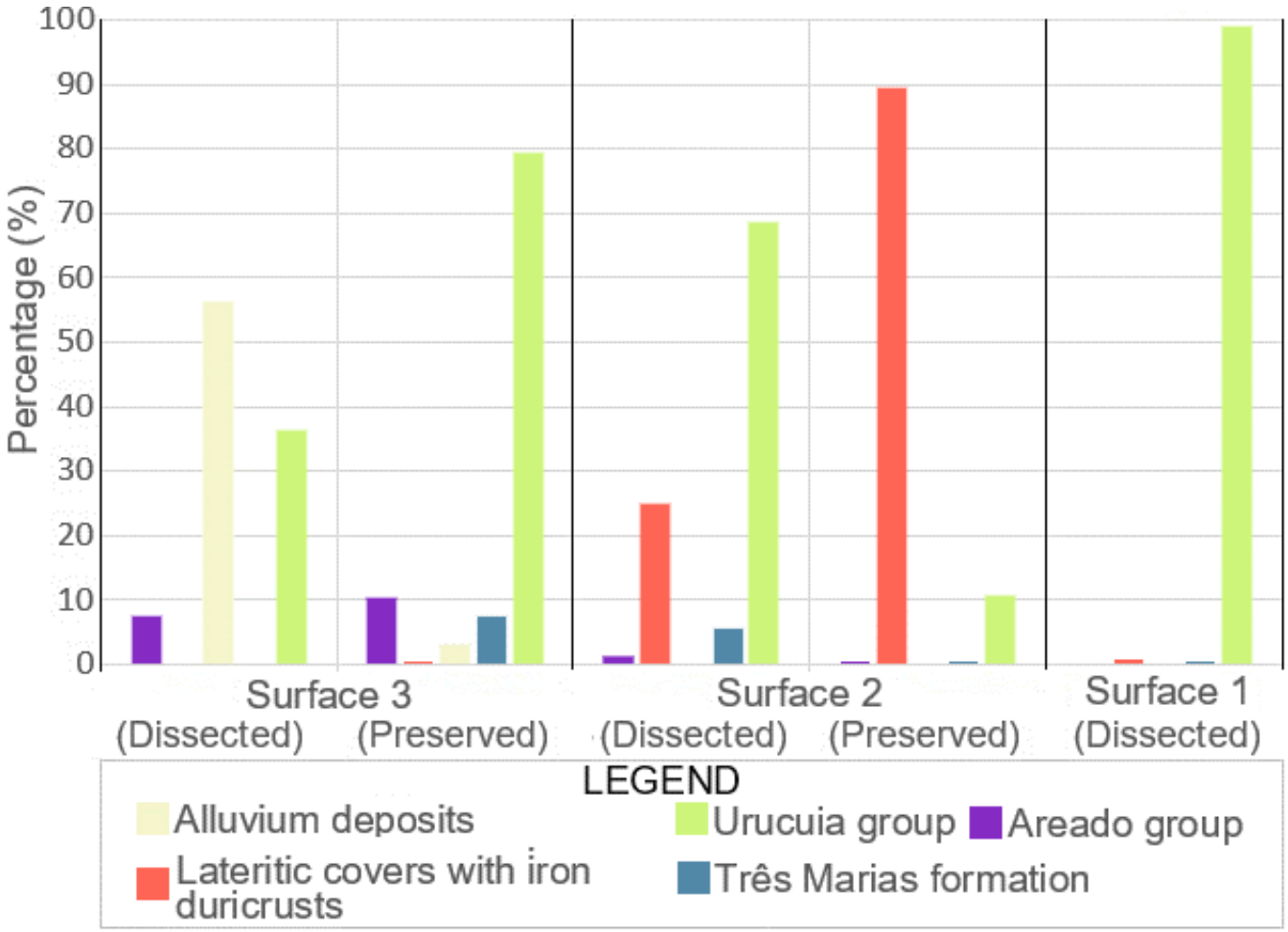

Figure 18. Graph of Relationship between the distribution of planation surfaces (preserved and dissected) and the distribution of geologic units.

5. Conclusions

In this work, a new algorithm was proposed to determine, without the need for interference from decision makers, planation surfaces from data obtained from radar images. The only parameter that must be provided for execution and calibration of the algorithm, the window size (in meters), is related to variation of number of pixels by the altitude and can be specified through pre-processing of database related to the study area. The accuracy of the algorithm, even with the filtering of the number of pixels, depends on the quality of the database used.

The method is based on the unsupervised classification of the frequency of elevation values for the pixels of an area, graphically represented. The preserved areas of the planation surfaces are indicated by higher frequency peaks in the graph and their dissected areas appears as valleys between the peaks. The sharper the peaks, the flatter/level is the planation surface. Otherwise, broader peaks suggest less flat and/or less level surfaces. The derivative provides the rate of change of the function for each altitude value, so the higher the value of the first derivative, the more pronounced the surface flatness. The greater the altimetric variation of DEMs, the better the precision of the results provided by the algorithm to distinguish the concavities of function, which represent the geometric signatures of the planation surfaces.

The landforms of the studied areas were associated to three planation cycles and correlated to the surfaces proposed by King (1956): *Velhas* Surface (the lowest in altitude and with low degree of flatness and leveling); South

American Surface (intermediate, with a high degree of flatness and leveling), and Post-Gondwana Surface (represented only by dissected forms located altimetrically above the level of South American Surface).

The mapped surfaces showed noteworthy correlation with soil types, indicating that the automated mapping of planation surfaces can help to understand the distribution of soil types in a region. The divergences found can be mainly attributed to the incompatibility of scales between the planation surface map and the soil map available for the studied area. More detailed soil maps and field-works would allow a better comparison of the distribution of mapped surfaces with the types of soils.

As the surface mapping is based on the altimetric stratification, the proposed method is best applied to regions with stepped planation levels and with tectonic stability, i.e., not significantly affected by orogenesis, differential epeirogenesis or tilting during or after the planation process. Results obtained for gently inclined planation surfaces, for surfaces controlled by local or regional base levels, and for hilly areas considered in (or close to) dynamic equilibrium must be interpreted with attention. Further studies must apply the algorithm to different regions and scales. Data from different DEMs may also be tested and compared.

The proposed algorithm can be used as a computational tool for guiding geomorphological, pedological and landscape mapping, specially at regions of difficult access.

Conflict of Interest: The authors declare no conflict of interest.

References

1. ALLARD, T. et al. Combined dating of goethites and kaolinites from ferruginous duricrusts. Deciphering the Late Neogene erosion history of Central Amazonia. Chemical Geology, v. 479, p. 136-150. https://doi.org/10.1016/j.chemgeo.2018.01.004.
2. AUGUSTIN, C.H.R.R.; MELO, D.R.; ARANHA, P.R.A. Aspectos Geomorfológicos de Veredas: um Ecossistema do Bioma do Cerrado, BRASIL. **Revista Brasileira de Geomorfologia**, v. 10, nº 1, 2009, p. 103-114.
3. BESSIN, P. GUILLOCHEAU, F. ROBIN, C. SCHROËTTER, J. BAUER, H. **Planation surfaces of the Armorican Massif (western France): Denudation chronology of a Mesozoic land surface twice exhumed in response to relative crustal movements between Iberia and Eurasia**. Geomorphology, Volume 233, 2015, Pages 75-91, ISSN 0169-555X. https://doi.org/10.1016/j.geomorph.2014.09.026.
4. BRAUN, O.P.G. **Contribuição à geomorfologia do Brasil Central.** Revista Brasileira de Geografia, Rio de Janeiro, 32(3):3-39, 1970.
5. BRASIL, Ministério das Minas e Energias. Secretaria Geral. **Projeto RADAMBRASIL**: Geologia, Geomorfologia, Pedologia, Vegetação e Uso potencial da terra. Folhas SD.23 - Brasília. Rio de Janeiro, 1977.
6. BURROUG, P.A.; VAN GAANS, P.F.M.; MACMILLAN, R.A. **High resolution landform classification using fuzzy-k means**. Fuzzy Sets and Systems, 113, 37-52, 2000. DOI: 10.1023/A:1013167712622.
7. COSTA, M. L. Aspectos geológicos dos lateritos da Amazônia. **Revista Brasileira de Geociências**, Curitiba, v. 21, n. 2, p. 146-160, 1991.
8. CPRM. **Mapa geodiversidade do Brasil:** influência da geologia dos grandes geossistemas no uso e ocupação dos terrenos. Brasília: CPRM, p. 68, 2006.
9. EMPRESA BRASILEIRA DE PESQUISA AGROPECUÁRIA – EMBRAPA. Sistema Brasileiro de Classificação de Solos. 5 ed. Rio de Janeiro: **Embrapa Solos**, p. 353, 2018.
10. EVANS, I. **General geomorphometry, In *Geomorphological techniques*, Goudie, A. (ed.):** British Geomorphological Research Group, London: Allen & Unwin: 31–37,1981.

11. EVANS, I.; DIKAU, R.; TOKUNAKA, E.; OHMORI, H.; HIRANOi, M. (eds). ***Concepts and modelling in geomorphology, international perspectives*, Tokyo,Japan:** TERRAPUB. 2003.
12. FREYSSINET, P.; THÉVENIAUT, H.; WYNS, R. **Dating of West African planation surfaces thanks to paleomagnetic approaches.** American Geophysical Union, Fall Meeting 2018. https://ui.adsabs.harvard.edu/abs/2018AGUFMEP23G2408F.
13. GOUDIE, A. ***Encyclopedia of Geomorphology***. London: Routledge, 2004, 1200 p.
14. GUILLOCHEAU, G..; SIMON, B.; BABY, G.; BESSIN, P.; ROBIN, C.; DAUTEUIL O. Planation surfaces as a record of mantle dynamics: The case example of Africa. Gondwana Research, Elsevier, 2018, 53, pp.82-98.
15. GUISAN, A.; WEISS, S.B.; WEISS, A.D. **GLM versus CCA spatial modeling of plant species distribution.** Kluweracademicpublishers. PlantEcol 143:107–122, 1999. https://doi.org/10.1023/A:1009841519580.
16. INMET. **Clima-Brasil**. Brasília, 2012. Disponível em: <http://www.inmet.gov.br/clima.phpt>.
17. JORDAN, G. **Morphometric analysis and tectonic interpretation of digital terrain data**: A case study. *Earth Surface Processes and Landforms*, *28*(8), 807-822. https://doi.org/10.1002/esp.469, 2003.
18. KING, L. **A geomorfologia do Brasil oriental**. Revista Brasileira de Geografia, Rio de Janeiro: IBGE. v. 2, n. 18, p. 147-265, 1956.
19. KRÖHLING, D. M. et al. **Planation Surfaces on the Paraná Basaltic Plateau, South America**. In: RABASSA, J.; OLLIER, C. D. (Eds.). Gondwana Landscapes in Southern South America: Argentina, Uruguay and Southern Brazil. [s.l.] Springer Earth System Sciences, p. 247–303, 2014. DOI:10.1007/978-94-007-7702-6.
20. LANZA, D.A. LADEIRA, F.B.S. Mapeamento, caracterização e correlação de superfícies de aplainamento no leste de Goiás, norte de Minas Gerais e oeste da Bahia. IN: **Anais XVI Simpósio Brasileiro de Sensoriamento Remoto** - SBSR, Foz do Iguaçu, PR, Brasil, INPE, 2013, pp. 3550-3556.
21. LIU, F., GAO, H., PAN, B. *et al.* Quantitative analysis of planation surfaces of the upper Yangtze River in the Sichuan-Yunnan Region, Southwest China. *Front. Earth Sci.* **13,** 55–74 (2019). https://doi.org/10.1007/s11707-018-0707-y.
22. LOUIS LEITHOLD,. **The Calculus with Analytic Geometry**. ISBN-10 : 0060441070; ISBN-13 : 9780060441074, 1989.
23. MACMILLAN, R.; PETTAPIECE, W.; NOLAN, S.; GODDARD, T. **A generic procedure automatically segmenting landforms into landform elements using DEMs, heuristic rules and fuzzy logic**. Fuzzy sets and Systems, 113, 81–109, 2000. https://doi.org/10.1016/S0165-0114(99)00014-7.
24. MARZIEH, M.; DINES, S. ***IOP Conf. Ser.:*** *Earth Environ. Sci.* **37** 012009, 2016.
25. MATHER, P. **Computer Processing of Remotely-Sensed Images**. Wiley, New York, p. 352, 1987.
26. MELO, D.R. As veredas nos planaltos do Noroeste Mineiro, caracterizações pedológicas e os aspectos morfológicos e evolutivos. **Master's Thesis** (Geography), Department of Geography and Regional Planning, Geosciences Institute, State University of São Paulo – UNESP, Rio Claro, SP, 1992, 218 p.
27. MELO, D.R. Evolução das Veredas Sob Impactos Ambientais nos Geossistemas Planaltos de Buritizeiro/MG. 2008. **Doctoral Thesis** (Geography), Geosciences Institute, Department of Geography, Federal University of Minas Gerais – UFMG, 2008, 341 p.
28. MEYBECK, M.; GREEN, P.; VOROSMARTY, C.J. **A New Typology for Mountains and Other Relief Classes: An Application to Global Continental Water Resources and Population Distribution**, Mount. Research & Development, 21, 34 – 45, 2001. https://doi.org/10.1659/0276-4741(2001)021[0034:ANTFMA]2.0.CO;2
29. MILIARESIS, G.; ARGIALAS, D. **Extraction & delineation of alluvial fans from DEMs & Landsat TM images**. *Photogrammetric Engineering &RemoteSensing*, **66**: 1093–1101, 2000.
30. MILIARESIS, G.; LLIOPOULOU, P. **Clustering of Zagros Ranges from the Globe DEM representation,** *Int. Journal of Applied Earth Observation &GeoInformation*, **5**: 17–28, 2004. https://doi.org/10.1016/j.jag.2003.08.001.

31. MILIARESIS, G.C. **Quantification of Terrain Processes.** In: Zhou Q., Lees B., Tang G. (eds) Advances in Digital Terrain Analysis. Lecture Notes in Geoinformation and Cartography. Springer, Berlin, Heidelberg, 2008. DOI: 10.1007/978-3-540-77800-4_2.
32. MMA/IBAMA/FUNATURA. **Plano de Manejo do Parque Nacional Grande Sertão Veredas.** Brasília: Funatura, 2003.
33. NIMER, E. **Climatologia do Brasil.** 2.ed., Rio de Janeiro: IBGE, 1989.
34. PETERSCHMITT, E.; FRITSCH, E.; RAJOT, J.L.; HERBILLON, A.J. 1996. Yellowing, bleaching and ferritisation processes in soil mantle of the Western Ghâts, South India. Geoderma, 74: 235-253. https://doi.org/10.1016/S0016-7061(96)00064-X.
35. QIN, C.Z.; ZHU, A.X.; SHI, X.; LI, B.L.; PEI, T.; ZHOU, C.H. **Quantification of spatial gradation of slope positions. Geomorphology 110:152–161.** https://doi.org/10.1016/ j. geomorph.2009.04.003, 2009.
36. RABASSA, J. Some Concepts on Gondwana Landscapes: Long-term landscape evolution, genesis, distribution and age. IN: RABASSA, J.; OLLIER, C. (Eds.) **Gondwana Landscapes in southern South America – Argentina, Uruguay and southern Brazil**, Dordrecht: Springer, 2014, pp. 35-46.
37. RADAMBRASIL. **Levantamento de Recursos Naturais Folha SD.23 Brasília: geologia, geomorfologia, pedologia, vegetação e uso potencial da terra.** Rio de Janeiro: Ministériode Minas e Energia. Secretaria Geral, v. 29, p.660, 1982.
38. SAADAT, H.; BONNELL, R.; SHARIFI, F.; MEHUYS, G.; NAMDAR, M.; ALEl-EBRAHIM, S. **Landform classification from a digital elevation model and satellite imagery**. Geomorphology, 100, 453–464, 2008. https://doi.org/10.1016/j.geomorph.2008.01.011.
39. SCHIMIDT, J.; HEWITT, A. **Fuzzy land element classification from DTMs based on geometry and terrain position.** Geoderma, 121, 243–256, 2004. https://doi.org/10.1016/j.geoderma.2003.10.008.
40. VASCONCELOS P.M.; RENNE P.R.; BRIMHALL G. H.; BECKER T. A. Direct dating of weathering phenomena by 39Ar-40~ and K-Ar analysis of supergene K-Mn oxides. **Geochim Cosmochim Acta** 58, 1994, 1635-1665.
41. VASCONCELOS, P. and CARMO, I. (2018). Calibrating denudation chronology through 40Ar/39Ar weathering geochronology. **Earth-Science Reviews**, 179, 411-435. doi: 10.1016/j.earscirev.2018.01.003.
42. VALADÃO, R. Geodinâmica de Superfícies de Aplainamento, Denudação Continental e Tectônica Ativa como condicionantes da Megageomorfologia do Brasil Oriental. Revista Brasileira de Geomorfologia. 10. 77-90. 10.20502/rbg. v10i2.132., 2009. DOI: http://dx.doi.org/10.20502/rbg.v10i2.132.
43. WANG, L.; LIU, H. **An Efficient Method for Identifying and Filling Surface Depressions in Digital Elevation Models for Hydrologic Analysis and Modelling**. International Journal of Geographical Information Science, 20, 193-213, 2006. https://doi.org/10.1080/13658810500433453.
44. LI-YANG XIONG, GUO-AN TANG, A-XING ZHU & YE-QING QIAN (2017) A peak-cluster assessment method for the identification of upland planation surfaces, International Journal of Geographical Information Science, 31:2, 387-404, DOI: 10.1080/13658816.2016.1205193.